

Lawrence Berkeley National Laboratory

Lawrence Berkeley National Laboratory

Title

Bulk band gaps in divalent hexaborides: A soft x-ray emission study

Permalink

<https://escholarship.org/uc/item/2446h5v8>

Authors

Denlinger, Jonathan D.
Gweon, Gey-Hong
Allen, James W.
et al.

Publication Date

2001-10-03

BULK BAND GAPS IN DIVALENT HEXABORIDES: A SOFT X-RAY EMISSION STUDY

J. D. DENLINGER

*Advanced Light Source, Lawrence Berkeley National Lab
Berkeley, CA 94720, USA
E-mail: JDDenlinger@lbl.gov*

G.-H. GWEON, J. W. ALLEN

*Randall Laboratory of Physics, University of Michigan
Ann Arbor, MI 48109-1120, USA*

A. D. BIANCHI[†], Z. FISK

*National High Magnetic Field Lab, Florida State University
Tallahassee, FL 32306, USA*

Abstract

Boron K-edge soft x-ray emission and absorption are used to address the fundamental question of whether divalent hexaborides are intrinsic semimetals or defect-doped bandgap insulators. These bulk sensitive measurements, complementary and consistent with surface-sensitive angle-resolved photoemission experiments, confirm the existence of a bulk band gap and the location of the chemical potential at the bottom of the conduction band.

1. Introduction

The discovery of weak itinerant ferromagnetism in certain divalent hexaborides^{1,2,3,4} provides strong motivation to determine the underlying electronic structure giving rise to the metallic carriers. One possibility predicted by LDA band calculations^{5,6}, and supported by the interpretation given to magneto-oscillatory studies^{7,8}, is a semi-metallic band overlap at the X-point of the cubic Brillouin zone, the absence of which would render stoichiometric material to be insulating. Several theoretical discussions^{9,10,11} presume the existence of such an overlap. As summarized elsewhere¹² we have recently given conclusive experimental proof that there is instead an X-point gap. This result eliminates all models that assume overlap and so may favor a ferromagnetic dilute electron gas picture¹³, but it also forces the consideration of boron vacancies as the origin of the electrons observed in nominally stoichiometric divalent materials, possibly favoring a picture in which the magnetic moments are car-

ried by boron vacancies¹⁴.

The X-point gap was first observed in angle resolved photoemission (ARPES) of EuB_6 and SrB_6 and ascribed by us initially only to the surface region probed in ARPES¹⁵. Strong motivation to reinterpret the ARPES result as showing a bulk gap¹⁶ was provided by a recent band calculation¹⁷ that includes a GW self energy correction and predicts CaB_6 to have the X-point band gap of 0.8 eV similar to that measured by ARPES. Results from bulk sensitive soft x-ray emission and absorption spectroscopy (SXE and XAS, respectively) showing the gap are an essential part of our experimental proof. This paper gives important aspects of the SXE/XAS results and analysis that were not presented previously.

2. Experimental

Single crystal hexaboride samples were grown from an aluminum flux using powders prepared by boro-thermally reducing cation oxides, a method shown to yield high quality with regard to

both structure and chemical composition¹⁸. Soft x-ray emission and absorption experiments were performed at the ALS Beamline 8.0.1 using the Tennessee/Tulane grating spectrometer. The experimental emission and absorption spectral resolutions were ≈ 0.35 eV and ≈ 0.1 eV, respectively. SXE, measured with a 1500 line/mm grating for fixed photon energy excitation at and above the B K-edge threshold, is used as a probe of the occupied boron partial density of states for dipole-allowed transitions back to the B 1s core-level, i.e. *p*-states. X-ray absorption, a probe of the unoccupied states, was measured both with total electron yield (TEY) as a function of photon energy and also with partial fluorescence yield (PFY) with the detection window covering the entire valence band emission. Differences between TEY and PFY signals arise from differing attenuation lengths and the experimental geometry which was set to 60° incidence excitation and 30° grazing emission relative to the sample surface. Absolute PFY energies were calibrated to published TEY spectra of the hexaborides¹⁹ and SXE spectra were calibrated to the excitation energy via the presence of elastic scattering in the emission spectra. Previous very early work on the hexaborides using electron-excited soft x-ray emission and thin film absorption measurements^{20,21} do not provide clear enough spectral detail at threshold to address the band gap issues that have only recently been raised.

3. Results

Fig. 1 shows a representative data set of soft x-ray emission and absorption at the boron K-edge for the divalent hexaborides. Very similar data to this example from a cleaved YbB₆ sample was also obtained for CaB₆, SrB₆, and EuB₆. Fig. 1(a) compares the two methods of measuring x-ray absorption, TEY and PFY. TEY, a measurement of the sample current, exhibits a sharp peak at ≈ 194 eV corresponding to a well-known B 1s \rightarrow 2p π^* transition¹⁹, which in part arises from surface layer oxidation of the air-cleaved sample. Also the absolute TEY signal exhibits a high background (removed in Fig. 1(a)) with declining slope due to the presence of lower energy absorption edges.

In contrast, the PFY signal, a measure of valence emission intensities integrated over the energy window shown in Fig. 1(b), does not exhibit the sharp TEY absorption peak due to a greater bulk emission sensitivity than the excitation depth which rapidly decreases while scanning through the absorption resonance. Also the valence band PFY signal inherently has zero pre-threshold intensity and hence is preferred over TEY for careful measurement of the threshold region. The PFY spectrum for YbB₆ shows a weak step-like threshold onset at 187.1 eV which is highlighted by a logarithmic scale in the inset to Fig. 1(a). TEY also shows an intensity cusp at this energy, but only for cleaved surfaces with minimal surface contamination. We interpret this threshold onset in the PFY spectrum as the energy position of the chemical potential which we define at the half-step intensity. Such an interpretation is not rigorous but is often successful, as shown for the case here in the discussion below. This location of the chemical potential or Fermi-edge (E_F) in the conduction band is immediately important for electronic structure models and is consistent with negative Hall coefficient measurements indicating the presence of electron (and not hole) carriers in the bulk^{22,23}.

Valence band emission spectra, shown in Fig. 1(b) were acquired at selected photon energies indicated by arrows in Fig. 1. An elastic peak present in the emission spectra is resonantly enhanced at the B 1s \rightarrow 2p absorption peak and is used for calibration of the SXE energy scale to that of TEY and PFY spectra. Excitation at the selected peaks in the PFY/TEY spectra and far above threshold show similar valence band emission profiles with small variations in the relative intensities of at least six discernable peaks and shoulders. Threshold excitation on the other hand produces much larger variation in the relative intensities (and energies) of the different valence emission peaks (discussed in the next section). The elastic peak is also observed to be enhanced at threshold, thus providing a distinct marker of E_F for all the emissionspectra. The non-threshold SXE spectra, on the other hand, exhibit a strong non-metallic decay of intensity approaching E_F , in contrast to the weak step-onset in the PFY spectrum which implies a small

occupancy of states at E_F . A lack of clear SXE detection of such density of states near E_F could be due to too little occupancy, very weak boron p -character, and/or a poorer SXE resolution than the occupied bandwidth.

4. Comparison to band theory

A detailed comparison of the YbB₆ SXE and PFY spectra to both LDA and GW calculations, presented in Fig. 2, reveals a clear distinction between the band-overlap and band gap electronic structure models. Available partial density of states (DOS) calculations exist in the literature for SrB₆ only⁶ and the GW calculation was performed for CaB₆¹⁷. However, since experimental SXE bandwidths of all hexaborides are very similar and the theoretical bandwidths for a given calculation method are also similar between different hexaborides, the comparison of experiment to theory involving different divalent cations is justified.

Fig. 2(a) shows the combined SXE (194.1 eV excitation) and PFY spectra, which can rigorously be placed on a common photon energy scale because the valence screened core hole is the same for both spectra. The photon energy scale is shifted to place the PFY threshold at 0 eV, i.e. E_F for the theoretical LDA p -DOS for SrB₆, which is also shown. The relative SXE and PFY intensities have been scaled to match the theoretical DOS amplitudes above and below E_F . Boron s -DOS and cation d -DOS, not probed by these measurements, are strongest at -8 eV and above +5 eV, respectively. The corresponding k -resolved LDA band structure (for CaB₆) along Γ -X for these DOS, exhibiting a small band overlap at the X-point between the valence and conduction bands, is plotted in Fig. 2(b). A clear discrepancy between the energy position of the LDA occupied and unoccupied DOS with the experimental spectra is seen.

A rigid shift of the theoretical DOS to lower energy provides a better agreement with experiment. The overall occupied boron-block bandwidth and relative peak amplitudes are in good agreement with the LDA p -DOS. However, independent energy shifts of the occupied and unoccupied states (-0.8 eV and -0.5 eV, respectively)

is required to make best alignment to the 2.5-5 eV SXE and 3 eV PFY peaks (Fig. 2(c)). This suggests a relatively larger experimental energy separation between the valence and conduction bands than predicted by LDA and thus no X-point band overlap.

Fig. 2(d) shows the GW bands along Γ -X for CaB₆ exhibiting a band gap at the X-point. The GW band calculation predicted a 10% expansion of the boron-block bandwidth compared to LDA. However this larger GW bandwidth is not consistent with the bandwidths measured here by SXE or by ARPES¹² which are in better agreement with LDA. Hence for Fig. 2(d) the GW energy scale has been multiplied by 0.9 to match the LDA bandwidth, and then shifted to lower energy placing E_F at the bottom of the X-point conduction band consistent with the PFY measurement.

Since the divalent hexaboride conduction band minimum resides at the X-point, threshold excitation into these unoccupied states is expected to exhibit X-point k -selectivity in the emission process due to the lack of intermediate scattering paths to other lower energy k -points. Indeed, a favorable one-to-one correspondence can be made between the X-point band energies of the modified GW band calculation in Fig. 2(d) to the dominant peaks labeled (1-5) in the threshold-excited SXE spectrum plotted in Fig. 2(e). Most important for our goal of distinguishing band-overlap versus band-gap electronic structure is the identification of peak 1 as the boron-block valence band maximum at ≈ 1 eV below E_F . The threshold-excited YbB₆ SXE spectrum thus provides a direct quantification of the bulk bandgap to be 1.0 eV minus the energy that the conduction band dips below E_F , thus providing a firm basis for the reasoning set forth in Ref. 12.

5. Discussion

These soft x-ray measurements verifying the existence of a bulk band gap are complementary to our surface-sensitive ARPES measurements of the Γ -X band structure^{12,15} which provide a more detailed view of the X-point gap. The position of the chemical potential at the bottom of the con-

duction band is also qualitatively consistent with ARPES measurements of an electron pocket at the X-point. While excess electron concentrations at the surface can be explained by band bending and charge redistribution effects, excess electron carriers in the bulk forces one to confront the issue of off-stoichiometry defects, i.e. electron counting and band filling of the hexaboride band structure with the presence of a band gap predicts divalent materials to be insulators. A rigid covalently bonded boron sublattice with mobile cations is suggestive of cation vacancies only, i.e. hole carriers, inconsistent with Hall coefficient measurements. The presence of boron vacancies on the other hand appears to be a more natural source of excess electrons and such defects have even been recently shown theoretically to possess magnetic moments which may be highly relevant to the origin of the anomalous ferromagnetism in La-doped CaB_6 and other divalent hexaboride systems¹⁴.

We have also found from a combination of SXE/PFY and ARPES spectra^{12,24} that the X-point gap is absent for trivalent LaB_6 and mixed valent SmB_6 implying a non-trivial transformation from divalency to trivalency. Additionally a distinct anomalous deviation from Vegard's law exists in the $\text{Ca}_{1-x}\text{La}_x\text{B}_6$ series. Rather than a monotonic increase in lattice constant expected from the larger La^{3+} size, the lattice parameter at first shrinks to a minimum at $\approx 10\%$ La doping before increasing again at higher La-doping²⁵. This critical La concentration may be correlated with a crossover from band-gap to band-overlap X-point electronic structure.

6. Summary

Boron K-edge soft x-ray emission and absorption have been used to probe boron occupied and unoccupied partial density of states of the divalent hexaborides, with data from YbB_6 used as an example. The chemical potential is identified to be located at the bottom of the conduction states in the absorption spectra and comparison of the emission spectra to calculated LDA density of states is used to identify the energy of the valence band maximum to be ≈ 1 eV below the chemical potential. This result establishes the

existence of a bulk X-point band gap consistent with recent GW band calculations and rules out the band overlap model as a starting point for theories to explain the novel ferromagnetism in doped and undoped hexaborides.

Acknowledgments

This work was supported at U. of Michigan by the U.S. DoE under Contract No. DE-FG02-90ER45416 and by the U.S. NSF Grant No. DMR-99-71611. The ALS is supported by the U.S. DoE under contract No. DE-AC03-76SF00098.

References

- [†] present address: Los Alamos National Laboratory, Los Alamos, NM 87545
- 1. D. P. Young *et al.*, *Nature* **397**, 412 (1999).
- 2. P. Vonlanthen *et al.*, *Phys. Rev. B* **62**, 10076 (2000).
- 3. H. R. Ott *et al.*, *Physica B* **281-2**, 423 (2000).
- 4. T. Terashima *et al.*, *J. Phys. Soc. Jpn.* **69**, 2423 (2000).
- 5. A. Hasegawa and A. Yanase, *J. Phys. C, Solid State Phys.* **12**, 5431 (1979).
- 6. S. Massidda, A. Continenza, T. M. D. Pascale, and R. Monnier, *Z. Phys. B* **102**, 83 (1997).
- 7. R. G. Goodrich *et al.*, *Phys. Rev. B* **58**, 14896 (1998).
- 8. M. C. Aronson *et al.*, *Phys. Rev. B* **59**, 4720 (1999).
- 9. M. E. Zhitomirsky, T. M. Rice, and V. I. Anisimov, *Nature* **402**, 251 (1999).
- 10. L. Balents and C. M. Varma, *Phys. Rev. Lett.* **84**, 1264 (2000).
- 11. V. Barzykin and L. P. Gor'kov, *Phys. Rev. Lett.* **84**, 2207 (2000).
- 12. J. D. Denlinger *et al.*, *cond-mat/0107429*.
- 13. D. Ceperley, *Nature* **397**, 386 (1999).
- 14. R. Monnier and B. Delley, *cond-mat/0105210*.
- 15. J. D. Denlinger *et al.*, *cond-mat/000922*.
- 16. J. D. Denlinger *et al.*, *Bull. Am. Phys. Soc.* **46**, 1218 (2001).
- 17. H. J. Tromp *et al.*, *Phys. Rev. Lett.* **87**, 016401 (2001).
- 18. H. R. Ott *et al.*, *Z. Phys. B* **102**, 337 (1997).
- 19. J. J. Jia *et al.*, *J. Electron Spectrosc. Related Phenom.* **80**, 509 (1996).
- 20. I. I. Lyakhovskaya, T. M. Zimkina, and V. A. Fomichev, *Sov. Phys. Solid State* **12**, 138 (1970).
- 21. M. Okusawa, K. Ichikawa, T. Matsumoto, and

- K. Tsutsumi, *J. Phys. Soc. Jpn.* **51**, 1921 (1982).
 22. Z. Fisk *J. Appl. Phys.* **50**, 1911 (1979).
 23. J. M. Tarascon *J. Appl. Phys.* **51**, 574 (1980).
 24. S.-K. Mo *et al.*, cond-mat/0107203.
 25. A. D. Bianchi and Z. Fisk, unpublished.

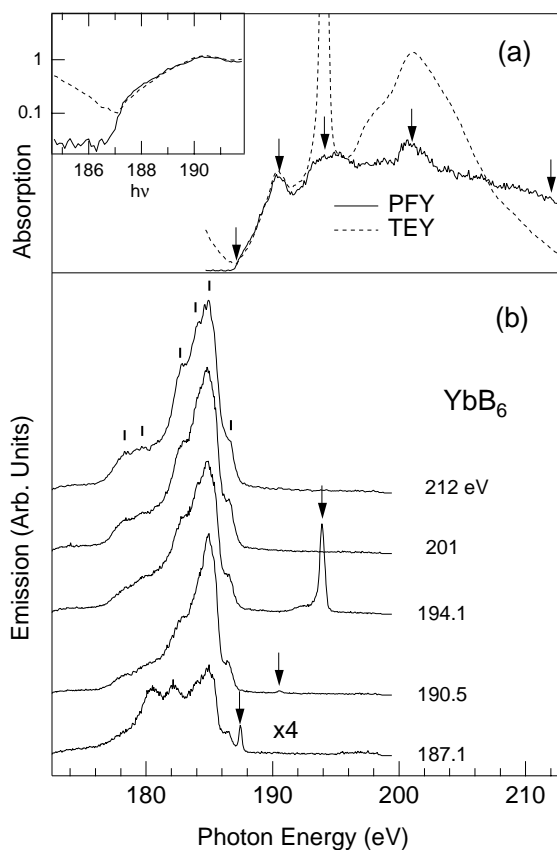


Fig. 1. Soft x-ray absorption (TEY, PFY) and emission (SXE) boron K-edge data set for YbB_6 . Arrows and values indicate the excitation energies. The logarithmic intensity scale of the inset highlights the step intensity onset of the PFY signal.

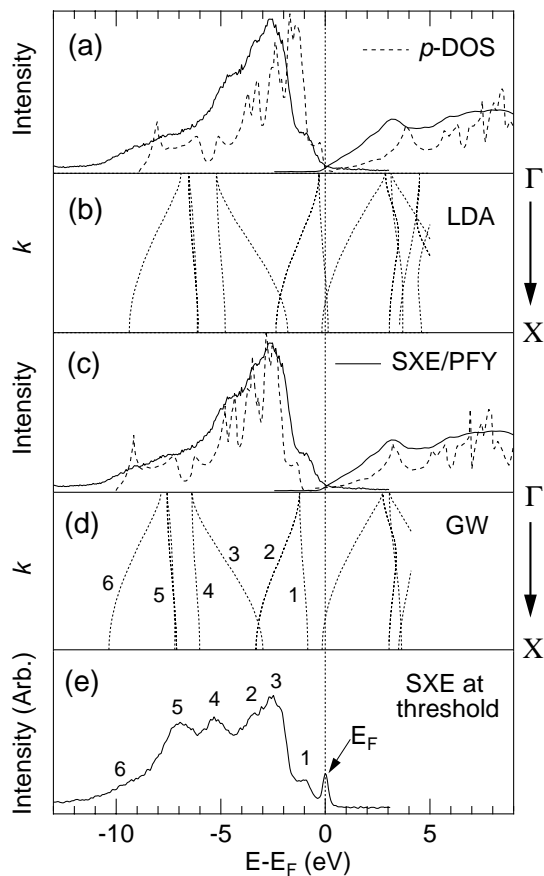


Fig. 2. (a) Comparison of YbB_6 SXE and PFY to LDA boron p -DOS for SrB_6 , (b) LDA band structure along Γ -X exhibiting band overlap at X, (c) comparison of SXE and PFY to energy shifted boron p -DOS, (d) GW band structure along Γ -X exhibiting a band gap, (e) YbB_6 SXE excited at threshold exhibiting X-point k -selectivity of peaks (1–5).